IOP PUBLISHING JOURNAL OF PHYSICS D: APPLIED PHYSICS

J. Phys. D: Appl. Phys. **41** (2008) 074029 (7pp) doi:10.1088/0022-3727/41/7/074029

Indentation and scratching mechanisms of a ZrCuAlNi bulk metallic glass

V Keryvin, R Crosnier[1], R Laniel[2], V H Hoang and J-C Sanglebœuf

LARMAUR, FRE-CNRS 2717, Université de Rennes 1, Campus de Beaulieu, 35042 Rennes, France

E-mail: vincent.keryvin@univ-rennes1.fr

Received 6 August 2007, in final form 28 September 2007
Published 12 March 2008
Online at stacks.iop.org/JPhysD/41/074029

Abstract

Indentation and scratching tests are carried out on a ZrCuAlNi bulk metallic glass. The bonded interface technique is used to characterize the plasticity mechanisms underneath the indentation. Finite-element analyses are conducted with a Drucker–Prager behaviour law to challenge the indentation experimental data. The relevance of the bonded interface technique, in terms of quantitative evaluation, is discussed. It is also reported that the angle value, for which radial bands intersect at the surface or underneath it, is not a constant value and depends on the indenter geometry. Finally, it is shown that a simple Drucker–Prager model can describe most of the indentation mechanical response but fails in predicting completely the indentation morphology.

(Some figures in this article are in colour only in the electronic version)

1. Introduction

Bulk metallic glasses (BMGs) have striking mechanical properties including large yield strains (∼2%) and high tensile strengths (up to 5 GPa [1]). However, submitted to classical uniaxial loadings, BMGs fail in an elastic-brittle way or quasi-brittle way [2]. Plastic deformation is highly localized in very thin shear-bands (10–100 nm thick). The investigation of the mechanisms of inelastic deformation is therefore precluded using uniaxial tests. In contrast, the sharp indentation test is a constrained deformation test where there is a possibility of studying the development of flow. Indentation has been extensively studied in BMGs. The load–displacement curve is monitored by means of instrumented indentation. In this case, the onset of pop-ins on that curve was correlated with the appearance of shear-bands around the indent after unloading [3, 4]. The question of observing or not observing shear-bands has also recently been addressed [5]. The nature and morphology of plastic deformation underneath the indenter has been studied by using the bonded interface technique [6–10]. The modelling of the mechanical response of metallic glasses during indentation has been made by showing that only a pressure-dependent (or normal-stress dependent) behaviour law, such as Drucker–Prager or Mohr–Coulomb, can match the experimental data [5,10–12]. In this study, pyramidal and conical indentation tests as well as scratching tests are carried out on a ZrCuAlNi BMG. The deformation mechanisms, at the surface and underneath it, are systematically investigated by using the bonded interface technique. Some features of existing correlations (plastic zone, normal-stress dependence) between experimental results and modelling are discussed. Finite-element simulations are also made to investigate how well a simple pressure-dependent model can match the different experimental data.

[1] Present Address: LMF, UMR-CNRS 6598, Ecole Centrale de Nantes, 1 rue de la Noë BP 92101, 44321 Nantes Cedex 3, France.

[2] Present Address: LMGC, UMR-CNRS 5508, Université Montpellier II, CC048 Place Eugéne Bataillon, 34095 Montpellier Cedex 05, France.

2. Experimental and numerical procedures

2.1. Experimental procedures

Indentation tests are performed on a $Zr_{55}Cu_{30}Al_{10}Ni_5$ (at.%) bulk metallic glass whose mechanical and physical properties are reported in table 1. Diamond conical (apex angles of 90° and 120°) and pyramidal (Vickers, Berkovich) indenters are used. Specimens are mirror-polished by standard metallographic techniques using SiC and diamond containing grids. Hardness is systematically computed by measuring the indentation dimensions by confocal microscopy. Plastic deformation mechanisms under the indenter are investigated

Table 1. Mechanical and physical properties of the $Zr_{55}Cu_{30}Al_{10}Ni_5$ BMG: d is the density measured by the Archimedes technique, E (Young's modulus) and ν (Poisson's ratio) are determined by ultrasonic echography, Y_t and Y_c are the yield stresses in tension and in compression, respectively [5], T_g is the glass transition temperature determined by thermal expansions measurements at 5 K min^{-1} [13].

d	E (GPa)	ν	Y_t (GPa)	Y_c (GPa)	T_g (K)
6.83	84.4	0.364	1.6	1.8	673

by the bonded interface technique [6, 7, 14] that is more adequate for BMGs either than direct *in situ* observation (non-transparency) or than post mortem observation after breaking an indented specimen along radial cracks like it is usually made for brittle ceramics (this BMG does not crack during indentation). Specimens are prepared by bonding two pieces together, already polished to a 1 μm finish, and are then clamped in a special device to reduce the bond thickness. Following this, the top surface of the bonded specimen is polished carefully so that the indentation face is flat. Vickers diamond indentations are performed on the bonded interface as well as away from it in the bulk for comparison. Indentations on the interface are conducted, for the Vickers pyramid, in such a way that either the indentation diagonals or the faces coincide with the interface, whose thickness is in the best cases 1–2 μm. For the Berkovich indenter, the indentations are performed so that either one diagonal and one face coincide with the interface or that two faces and the indenter tip coincide with the interface. Scratching behaviour is investigated using a laboratory-made device [15] either with a 90° conical indenter or with a Vickers indenter (diagonal oriented). For the first situation, a normal load is assigned from 0 to 4 N (0.1 N s^{-1}) with a translation rate of 10 or 100 μm s^{-1}. In the second case, a constant normal load of 1 or 2 N (0.1 N s^{-1}) at a rate of 100 μm s^{-1} is employed. The tangential load is recorded during the test and the apparent friction coefficient is calculated as the ratio tangential load to normal load. The observations are made by optical microscopy (Olympus BX60F-3), scanning electron microscopy (Jeol JSM 6301 F) and confocal microscopy (Leica ICM1000).

2.2. Numerical procedures

Simulations, by finite-element analysis (FEA), of the indentation response of BMGs are undertaken using three-dimensional (3D) conditions (for the Berkovich and Vickers indenters). The software used is the freeware Cast3M [16] developed by the French Atomic Energy Agency. A planar mesh is first made; it is composed of 2,073 four-noded quadrilateral elements with a coarse meshing far from the indentation zone and a finer meshing beneath the indenter. This mesh is then used as a a starting surface then rotated at 60° (Berkovich) or 45° (Vickers) because the two pyramids (Berkovich and Vickers) have symmetries so that only 1/6th (respectively 1/8th) of them could be meshed. The resulting elements are 13,428 eight-noded prisms except along the axis where six-noded pyramidal elements were used. All simulations are displacement controlled. At least 30 elements are in contact with the indenter at maximum load. The size of the mesh is chosen to be insensitive to the far-field boundary conditions. In all simulations the finite deformation formulation is used. Two pyramidal indenters (Berkovich and Vickers) are used. A linear isotropic elastic behaviour is assumed with a very high Young's modulus of 1100 GPa and a Poisson's ratio of 0.07 for the diamond indenters. The contact between the indenter and the alloy follows an associated Coulomb's law of friction with a friction coefficient of 0.2. An associative elasto-perfectly-plastic Drucker–Prager behaviour law is used for the BMG with elasticity parameters and yield strengths experimentally assessed (see table 1). For all simulations, hardness is computed by measuring the surface profiles at a full applied load.

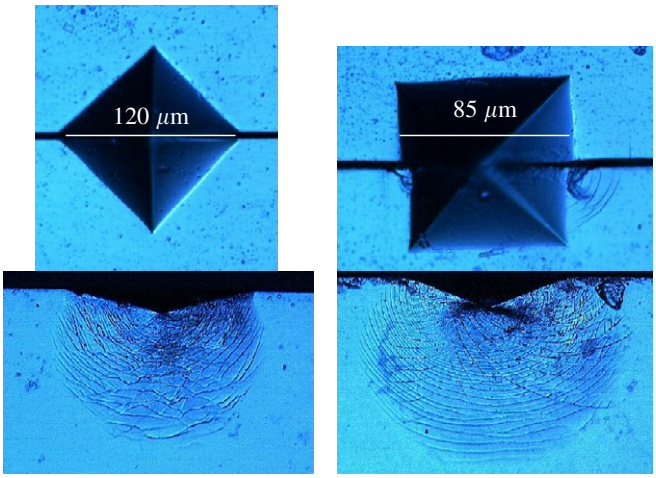

Figure 1. Optical micrographs of a 5 kg Vickers indentation on the bonded interface. (*a*) Along the diagonals: above (top) and underneath (bottom). (*b*) Along the faces: above (top) and underneath (bottom).

3. Results

3.1. Vickers indentations

The hardness of this alloy under Vickers indentation is found to be 5.1 GPa. Figure 1 shows the surface and the sub-surface deformation of the alloy under a 5 kg Vickers indentation on a bonded interface. Two configurations are chosen: the first one, referred to as 'along the diagonals', consists of aligning the indenter with the interface so that the two corners (diagonals) of the indenter coincide with the interface; the second one, referred to as 'along the faces', consists of aligning the indenter with the interface so that the two faces of the indenter coincide with the interface. No shear-bands are observed under usual conditions (figure 1(*a*) top) at the surface in the bulk. In (figure 1(*b*) top), a small perturbation due to the interface causes some shear-bands to appear. The slight convexity of the faces (compared with a perfectly square indentation) is due to the piling-up (see figure 2(*b*)). The sub-surface plastic deformation zone seems quasi-semi-circular in shape under the faces (figure 1(*b*) bottom) and contains a high density of shear-bands. In no case were cracks observed within the deformed zone. In figure 1(*a*) (bottom), the plastic zone is

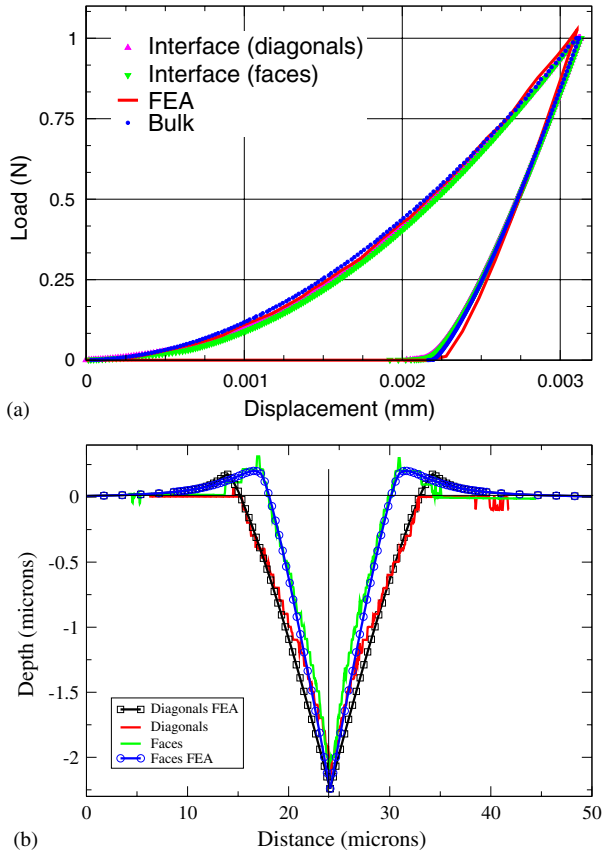

Figure 2. A 1 N Vickers indentation experiment: (*a*) load–displacement curves; comparisons between experimental data (in the bulk and on the bonded interface) and numerical simulations (FEA); (*b*) residual indentations (diagonals and faces), comparison between experimental data and numerical simulations (FEA).

hemispherical with its centre under the free surface and even under the indentation tip. Within the deformation zone, two morphologically distinct shear-bands are seen: semi-circular ones and radial ones. There is a higher density of radial bands underneath the faces of the Vickers indenter than underneath its diagonals. Moreover, the tendency of bands to curve towards the surface and to nearly reach it is evidenced for the faces while for the diagonals it is far less pronounced. Finally, the radial bands intersect at a given included angle. This angle varies from 84° to 99° for both configurations with a mean value of 90.2°. A comparison of a 1 N Vickers indentation, between experimental data and numerical simulations, is presented in figure 2. In figure 2(*a*), the load–displacement curve in the bulk, that is the mechanical response of the indentation test, is very well predicted by the pressure-dependent Drucker–Prager model (FEA), only by taking the elasticity parameters and the compressive and tensile yield strengths. The experimental curves corresponding to indentations on the interface (along the diagonals and the faces) are added in this figure, showing the same mechanical response. In figure 2(*b*), the cross-sections of the residual indentation (1 N Vickers indentation observed by confocal microscopy) along the diagonals and the faces are both plotted. As remarked before, the cross-section along the faces shows a pile-up while none can be evidenced along the diagonals. A comparison is made with the FEA. Along the faces, the residual geometry is very well predicted including the pile-up. In contrast, even if the residual shape along the diagonals is also well predicted, a pile-up (smaller than along the faces) is simulated while none is observed experimentally.

3.2. Berkovich indentations

The hardness of this alloy under Berkovich indentation is found to be 5.4 GPa. Figure 3 shows the surface and the sub-surface deformation of the alloy under a 1 N Berkovich indentation on the bonded interface. Two configurations are chosen: the first one, referred to as 'diagonal-to-face', consists of aligning the indenter with the interface so that a diagonal and a face of the indenter coincide with the interface; the second one, referred to as 'face-to-face', consists of aligning the indenter with the interface so that two faces and the tip of the indenter coincide with the interface. Semi-circular shear-bands are always observed around the faces (figures 3(*a*) and (*b*) top) at the surface and the interface indentations look perfectly like bulk ones. The slight convexity of the faces (compared with a perfectly triangular indentation) is due to the piling-up (evidenced by the Nomarski contrast then that is sensitive to height changes), which is more pronounced than that on the faces of a Vickers for the same load.The sub-surface plastic deformation zone looks no longer symmetric underneath the edge-to-face indentation (figure 3(*a*) bottom) and looks symmetric underneath the diagonal-to-face indentation (figure 3(*b*) bottom). As in the Vickers case, semi-circular and radial bands are observed but the former ones are incomplete in the diagonal-to-face case. There is a higher density of radial bands underneath the face-to-face indentation than underneath the diagonal-to-face one. The tendency of bands to curve towards the surface observed under the faces of the Vickers indentation is not seen here. The radial bands do not intersect underneath the diagonal-to-face indentation. In the other case, they do it at an included angle of around 101°.

A comparison of a 1 N Berkovich indentation, between experimental data and numerical simulations, is presented in figure 4(*a*). The load–displacement curve is very well predicted by the pressure-dependent Drucker–Prager model in the loading part as well as in the beginning of unloading. The last part of unloading, and especially the residual depth, is, in contrast to the Vickers case, not well predicted. The experimental curves corresponding to indentations on the interface are added in this figure, showing the same mechanical response.

3.3. Conical indentations

A typical indentation of a 90° conical indentation is shown in figure 4(*b*). As already reported [5], shear-bands are always seen around the indentation in two types: circular bands and radial bands in a logarithmic spiral shape. These latter bands intersect at an included angle of around 94°. A similar study was made with a 120° cone giving an angle of 90°.

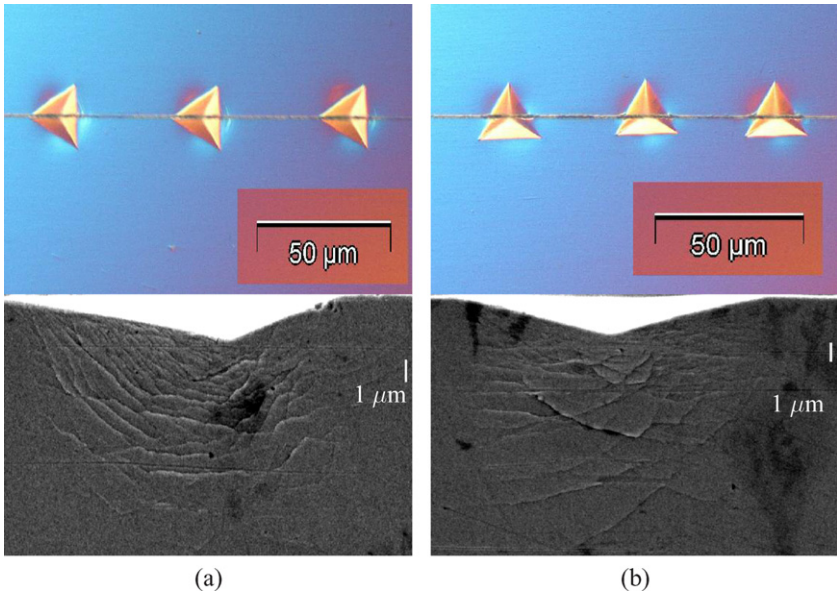

Figure 3. Optical and SEM micrographs of a 1 N Berkovich indentation on the bonded interface. (*a*) Diagonal-to-face configuration: above (top) and underneath (bottom). (*b*) Face-to-face configuration: above (top) and underneath (bottom).

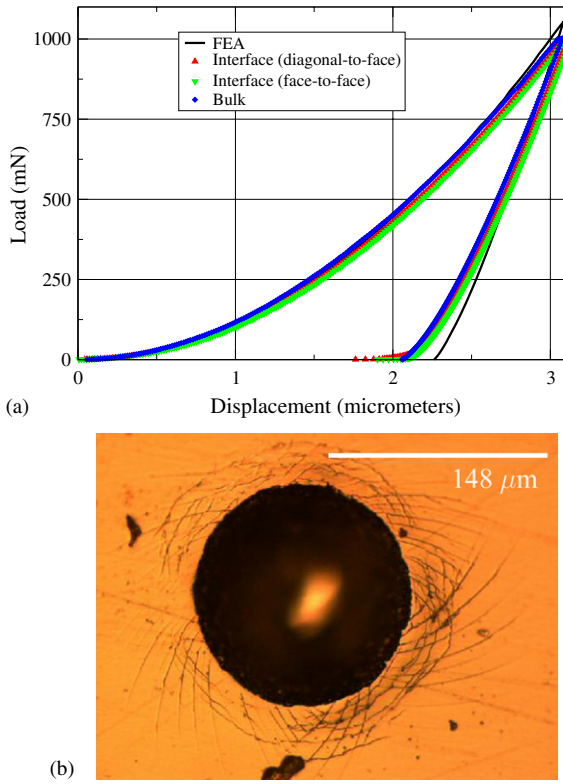

Figure 4. (*a*) Load–displacement curves for a 1 N Berkovich indentation; comparisons between experimental data (in the bulk and on the bonded interface) and numerical simulations (FEA). (*b*) A 100 N 90° conical indentation.

3.4. Scratching behaviour

A typical scratch is shown in figure 5. The indenter has created a groove that gets wider as the normal load is increased (here from 0 to 4 N). A closer look (insets 1 and 2) shows the presence of a large number of shear-bands on the sides of the groove. These bands are remarkably oriented vis-à-vis the groove and opposite to the scratching direction. For all cases (the two different indenters and the two translation rates), this angle lies between 40° and 60°. With the increase in the normal load, this inclination is the same but the density of shear-bands increases (the distance between two bands decreases). When the load is even higher, a chip is even formed (see inset 3). The apparent friction coefficient is 0.65 for the Vickers indenter and 0.5 for the conical one below 2 N; it increases up to 0.65 (when chips are formed) at 3 N and then keeps constant.

A comparison between a Vickers indentation and a Vickers scratch is made in figure 6. Under the scratch, no semi-circular shear-bands are observed. Only radial shear-bands are seen. These have a tendency to curve towards the surface and to nearly reach it. They intersect at a given included angle of 80°.

4. Discussion

4.1. Bands at the surface

The condition for bands to be observed at the surface has already been addressed [5]. They are only observed when the indenter is sharp enough to leave the elasto-plastic regime of indentation and reach the fully plastic one. For the Zr-based alloy considered here, the Vickers indenter is not sharp enough. Only perturbations of the test, such as the bonded interface or an imperfect normality between the indenter and the material, can cause bands to appear around the faces of Vickers indentations, often in an asymmetric way. In contrast, sharper indenters such as a 90° cone or a Berkovich pyramid cause bands to be seen at the surface in a symmetric way. The bonded interface technique allows to investigate underneath the indenter which mechanisms are responsible for these bands. As will be recalled later, the semi-circular shear-bands are artefacts due to the bonded interface and only radial bands are mechanisms that exist during bulk indentation. So the bands

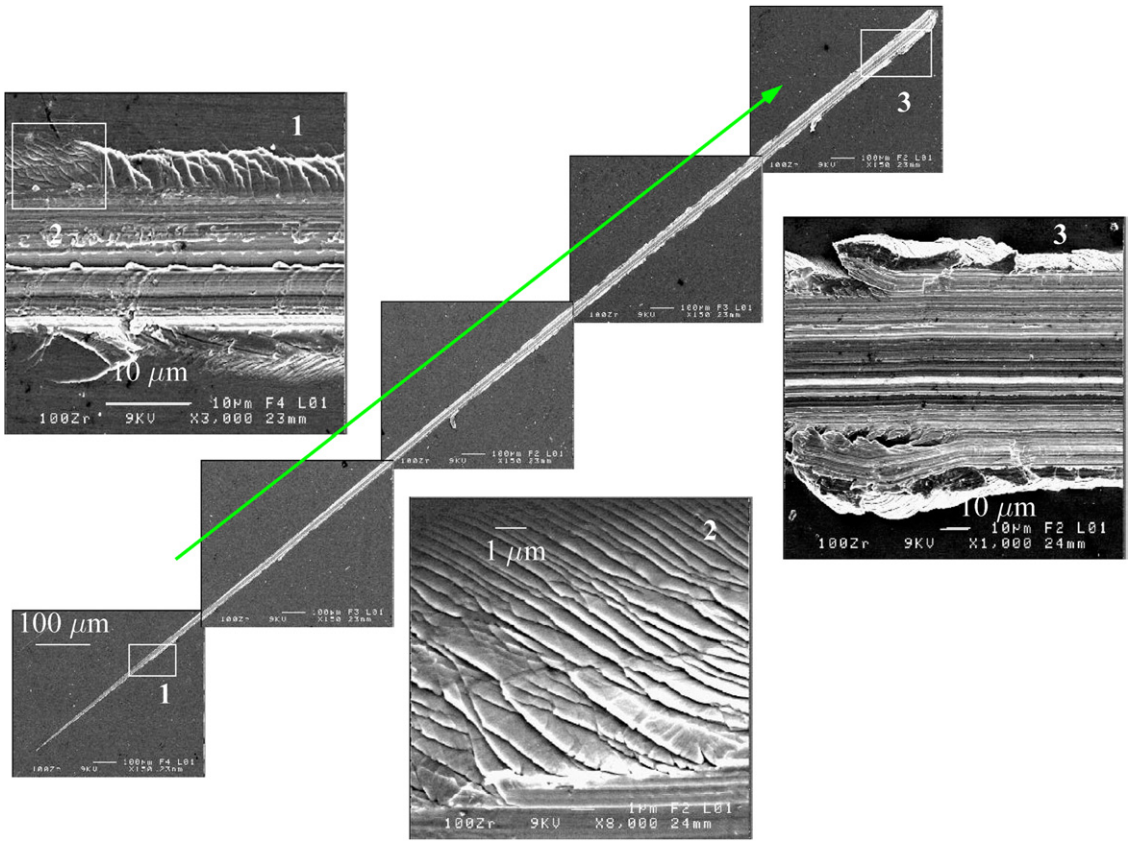

Figure 5. SEM micrographs of a 90° conical scratch (normal load from 0 to 4 N; 0.1 N s^{-1}) at a constant translation rate of 10 μm s^{-1}. The arrow shows the translation direction and insets are higher magnification zones.

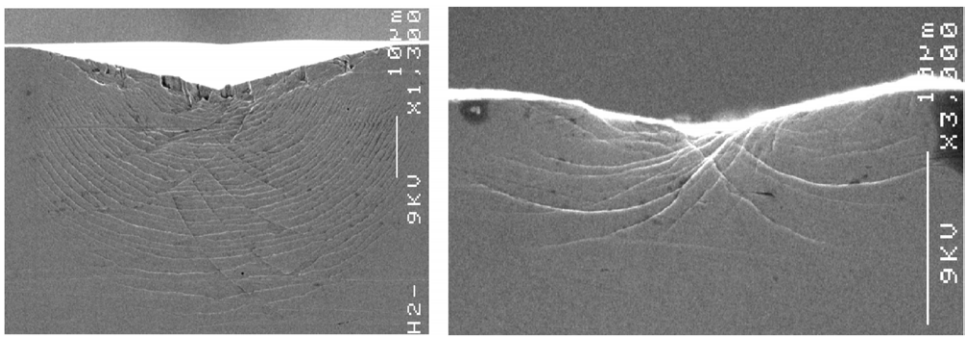

(a) (b)

Figure 6. Comparisons of the deformation morphology under (*a*) a 2.94 N Vickers indentation along the diagonals and (*b*) a 2 N Vickers scratch along the diagonals.

seen at the surface are radial bands that reach the free surface (they do not reach it with the bond) and not semi-circular bands.

4.2. Intersection of bands and normal-stress sensitivity of flow

The question of pressure-sensitivity of flow in metallic glasses, by means of indentation techniques, has been addressed in the literature in several ways. The mechanical response, that is the load–displacement curve, is not well predicted by a pressure-independent behaviour law while a contribution of normal-stress (Mohr–Coulomb) or pressure terms (Drucker–Prager) gives accurate results *vis-à-vis* experimental data [5, 11, 12]. The constraint factor (that is the ratio of hardness to the compressive yield strength) was also found to be higher for metallic glasses [5,8] than for pressure-independent materials, in the fully plastic regime of indentation. The dependence of the constraint factor, in the elasto-plastic regime of indentation, on the indentation strain has been very well predicted using a Drucker–Prager model [5, 12]. The hardness values that depend on the indenter geometry in the elasto-plastic regime have been correctly evaluated using FEA, for spherical, conical and pyramidal geometries, with a Drucker–Prager model [5]. A last feature concerns the angle for which radial shear-bands intersect either on the surface for axisymmetric indenter geometries or underneath the indentation for all geometries. A

number of authors have correlated the deviation of this angle from the maximum shear stress angle of 90° to a normal-stress dependence (see, e.g. [9,10,12,17,18]). In our case by varying the indenter geometries (two different apex angle cones) and by using the bonded interface technique to look at the intersecting angle underneath the indentation or the groove, no consistent value was found. It is believed that one must be very cautious when linking this angle to the normal-stress dependence.

4.3. Relevance of the bonded interface technique

Comparisons of the load–displacement curves in the bulk and on the interface (when this latter is thin enough), see figure 2(*a*) and figure 4(*a*), show that the plastic (area under the loading and unloading curves), total (area under the loading curve) and elastic (difference between the total energy and plastic energy) energies are the same. Therefore it is suggested that the mechanisms during an indentation on the bonded interface should be very similar to the ones taking place in the bulk. However, the deformed zone underneath the indentation can be seen by tilting the specimen in the SEM. It is evidenced that the plastic flow of the BMG occurred into the softer and more compliant interface than the BMG. The corresponding plastic bulge is serrated and contains both the semi-circular shear-bands that are out-of-plane shear displacements and the radial bands that are a result of in-plane shear displacements [8]. The radial bands are believed to be plane strain features that appear in the bulk while radial bands are more plane stress features (as with a free surface) which are artefacts. Ramamurty *et al* [8] also suggested that the deformation through in-plane shear displacements occurs after out-of-plane deformation.

The question of the relevance of the bonded interface technique for describing the indentation mechanisms is at stake. As the semi-circular bands dissipate a very important fraction of plastic energy, what would be the morphology of the radial shear-bands if they were to dissipate all of the plastic energy? In particular a higher density of bands, higher lengths or more plastic strain accumulated are reasonable scenarios. Therefore, quantitative evaluations of the BMG plasticity via observations of the bonded surfaces can be highly misleading. For instance, the plastic zone shape and dimensions should not be taken for granted.

The deformation zone underneath a scratch groove does not show any semi-circular band because the tangential load lays sufficient stress so that contact is made between the two polished surfaces and the compliant bond must play a minor role in that case. More confidence must be put on that case; however no direct link with what really takes place under an indenter can be made.

4.4. Indentation versus scratching mechanisms

The question of the comparison of indentation and scratching mechanisms is only partially addressed in this paper. It is obvious that scratching is a more severe deformation mode than indentation for the same normal load: the influence of the tangential load, and therefore friction, and also the translation rate are, among others, factors that may contribute to the differences in the plastic deformation mechanisms. Nevertheless, striking differences are to be mentioned. With the Vickers indenter, no bands are seen around the indentations after indentation while a high number of bands are observed along the scratch groove. With the conical indenter, many more bands are seen during scratching than during indentation. It means that, for the same load, scratching is more likely able to make the material enter the fully plastic regime of indentation. Moreover, the higher the load, the higher the number of bands at the surface, to accommodate plastic deformation.

4.5. Relevance of the behaviour law for FEA

As reported before, a pressure-dependence of flow is necessary to adequately describe the indentation response of metallic glasses. If the load–displacement curve is very well described for the Vickers indenter and relatively well described for the Berkovich indenter, three topics are of concern. First, the last unloading part for the Berkovich indenter is badly described. Secondly, a perfectly plastic behaviour, like the one used, will simulate piling-up on the diagonals, by even taking a higher friction coefficient, which is suggested by the apparent friction coefficients found by scratching tests. To reduce this pile-up, one must either introduce some strain-hardening, which is not experimentally proved for BMGs, or change the flow rule to a non-associativity. Finally, even if the load–displacement curve is very well simulated, it constitutes only one piece of a jigsaw to state that a correct mechanical description has been made. As an example, the load–displacement curves are nearly the same experimentally in the bulk and on the interface while it was shown that different mechanisms are at stake. A behaviour law that fits some experimental data must be challenged in other mechanical experiments to make it more relevant. Recently, Anand and Su [10, 19] proposed a Mohr–Coulomb behaviour law in finite deformations with an non-associative flow rule depending on the stress state. They compared FE simulations with several experimental tests and reported very good agreement with the mechanical responses as well as with the intersecting angle in-plane strain indentation. This kind of modelling seems to be a good response to the complexity of the mechanical description of flow in metallic glasses.

5. Conclusion

Conical and pyramidal indentation tests as well as scratching tests were carried out on a ZrCuAlNi bulk metallic glass and the bonded interface technique was used to systematically monitor and study the plasticity mechanisms. Three main conclusions can be drawn and extended to other amorphous alloys, at least Zr- or Pd-based ones. First, even if the bonded technique is very useful for hints on what takes place during indentation, its limitations concern the quantitative interpretation one can give, for example, on the plastic zone morphology and size. In contrast, more confidence may be put on the scratching mechanisms investigated with this technique. Secondly, the correlation between the angle value, for which radial shear-bands intersect in axisymmetric cases or underneath the indentation, and a normal-stress dependence of flow is shown to be not obvious. Finally, using an associative

pressure-dependent model such as the Drucker–Prager one (with only the elastic and yield strengths parameters), even if it leads to very good description, is not sufficient to capture all the indentation features.

Acknowledgments

VK would like to thank Dr M-L Vaillant, University of Rennes, France, for her experimental assistance, Professor Y Yokoyama, Tohoku University, Japan, for providing the specimens and J Le Lannic (CMEBA, University of Rennes) for the SEM pictures.

References

[1] Inoue A, Shen B L, Koshiba H, Kato H and Yavari A R 2004 Ultra-high strength above 5000 MPa and soft magnetic properties of Co–Fe–Ta–B bulk glassy alloys *Acta Mater.* **52** 1631

[2] Zhang Z F, Eckert J and Schultz L 2003 Difference in compressive and tensile fracture mechanisms of $Zr_{59}Cu_{20}Al_{10}Ni_8Ti_3$ *Acta Mater.* **51** 1167

[3] Golovin Y I, Ivolgin V I, Khonik V A, Kitagawa K and Tyurin A I 2001 Serrated plastic flow during nanoindentation of a bulk metallic glass *Scr. Mater.* **45** 947

[4] Schuh C A, Argon A S and Nieh T G 2003 The transition from localized to homogeneous plasticity during nanoindentation of an amorphous metal *Phil. Mag.* **83** 2585

[5] Keryvin V 2007 Indentation of bulk metallic glasses: relationships between shear-bands observed around the prints and hardness *Acta Mater.* **55** 2565–78

[6] Jana S, Ramamurty U, Chattopadhyay K and Kawamura Y 2004 Subsurface deformation during Vickers indentation of bulk metallic glasses *Mater. Sci. Eng.* A **375–377** 1191

[7] Jana S, Bhowmick R, Kawamura Y, Chattopadhyay K and Ramamurty U 2004 Deformation morphology underneath the Vickers indent in a Zr-based bulk metallic glass *Intermetallics* **12** 1097

[8] Ramamurty U, Jana S, Kawamura Y and Chattopadhyay K 2005 Hardness and plastic deformation in a bulk metallic glass *Acta Mater.* **53** 705

[9] Zhang H, Jing X, Subhash G, Kecskes L J and Dowding R J 2005 Investigation of shear band evolution in amorphous alloys beneath a Vickers indentation *Acta Mater.* **53** 3849

[10] Su C and Anand L 2006 Plane strain indentation of a Zr-based metallic glass: experiments and numerical simulation *Acta Mater.* **54** 179

[11] Vaidyanathan R, Dao M, Ravichandran G and Suresh S 2001 Study of mechanical deformation in bulk metallic glass through instrumented indentation *Acta Mater.* **49** 3781

[12] Patnaik M N M, Narasimhan R and Ramamurty U 2004 Spherical indentation response of metallic glasses *Acta Mater.* **52** 3335

[13] Keryvin V, Vaillant M-L, Rouxel T, Gloriant T and Kawamura Y 2002 Thermal stability and crystallisation of a $Zr_{55}Cu_{30}Al_{10}Ni_5$ bulk metallic glass studied by in situ ultrasonic echography *Intermetallics* **10** 1289

[14] Guiberteau F, Padture N P and Lawn B R 1994 Effect of grain size on hertzian contact damage in alumina *J. Am. Ceram. Soc.* **77** 1825

[15] Le Houérou V, Sangleboeuf J C, Dériano S, Rouxel T and Duisit G 2003 Surface damage of soda-lime-silica glasses: indentation scratch behavior *J. Non-Cryst. Solids* **316** 53

[16] http://www-cast3m.cea.fr/cast3m/index.jsp

[17] Tang C, Li Y and Zeng K 2006 Characterization of mechanical properties of a Zr-based metallic glass by indentation techniques *Mater. Sci. Eng.* A **304** 215–23

[18] Trichy G R, Scattergood R O, Koch C C and Murty K L 2005 Ball indentation tests for a Zr-based bulk metallic glass *Scr. Mater.* **53** 1461

[19] Anand L and Su C 2005 A theory for amorphous viscoplastic materials undergoing finite deformations, with application to metallic glasses *J. Mech. Phys. Solids* **63** 1362–96